Electronic Supplementary Material (ESI) for Environmental Science: Nano.

Supporting Information (SI) on

Experimental and Theoretical Evidence for Competitive Interaction of Tetracycline and Sulfamethazine on Reduced Graphene Oxides

Wencheng Song,[ab] Tongtong Yang,[c] Xiangxue Wang,[d] Yubing Sun,[d*] Yuejie Ai,[a*] Guodong Sheng,[a] Tasawar Hayat,[e] Xiangke Wang[aef*]

[a] *School of Environment and Chemical Engineering, North China Electric Power University, Beijing 102206, P. R. China*

[b] *Center of Medical Physics and Technology, Hefei Institutes of Physical Science, Chinese Academy of Sciences, Hefei 230031, P. R. China*

[c] *University of Science and Technology of China, Hefei, 230026, P. R. China*

d *Institute of Plasma Physics, Hefei Institutes of Physical Science, Chinese Academy of Science, Hefei, 230031, P.R. China*

[e] *Collaborative Innovation Center of Radiation Medicine of Jiangsu Higher Education Institutions and School for Radiological and Interdisciplinary Sciences, Soochow University, 215123, Suzhou, P.R. China*

[f] *NAAM Research Group, Faculty of Science, King Abdulaziz University, Jeddah 21589, Saudi Arabia*

*: Corresponding authors. Email: sunyb@ipp.ac.cn (Y. Sun); aiyuejie314@126.com (Y. Ai); xkwang@ipp.ac.cn or xkwang@ncepu.edu.cn (X. Wang); Tel: +86-10-61772890; Fax: +86-10-61772890.

Submitted to Environmental Science & Technology

Supplemental Information, 14 pages with 4 Figures and 6 Tables

Synthesis of Reduced Graphene Oxides (rGOs). The rGOs were synthesized by hydrazine hydrate ($H_2N\text{-}NH_2{\cdot}H_2O$) reduction of GOs under water-cooled condenser conditions.[S1] Firstly of all, GOs were synthesized by using modified Hummers method.[S2] Briefly, 1.0 g graphite, 1.0 g $NaNO_3$, and 40 mL H_2SO_4 were mixed in an Erlenmeyer flask under mechanical stirring and ice-water bath conditions, and then 6.0 g $KMnO_4$ was slowly added into suspensions. Then the mixture was reacted at 20 ± 1 ^oC for 5 days. Later, 85 mL Milli-Q water was added into the mixture. The solution was stirred for 30 min at 90 ± 1 ^oC, and then cooled to 60 ^oC. 6 mL H_2O_2 (30 %) was added slowly to remove the residual MnO_4^-. The GOs suspension was obtained by the collection of supernatant after ultrasonic treatment (140 w) for 30 min and centrifugation at 9000 rpm for 10 min. The solution was filtered and rinsed with Milli-Q water thoroughly, and the GOs powder was obtained through filtration and freeze drying overnight.

The rGOs were obtained by $H_2N\text{-}NH_2{\cdot}H_2O$ reduction of GOs under water-cooled condenser conditions. Briefly, 0.1 g of GOs were dispersed in 100 mL of deionized water under ultrasonication (150 W) until it became clear with no visible particulate matter. Then 1.0 mL 32.1 mmol/L $H_2N\text{-}NH_2{\cdot}H_2O$ was added into the dispersion under water-cooled condenser conditions, and mixtures were vigorously heated at 100 °C for 24 h under vigorous stirring conditions. The yellow-brown solution was gradually transferred to black precipitate during the reduction process.

Batch Adsorption Experiments. Adsorption kinetic experiments were carried out to estimate the adsorption rates of TC and SMZ and the equilibrium time required to obtain the adsorption isotherms. Briefly, certain amounts of rGOs, TC and SMZ were mixed in glass vials (total 10 mL, m/v = 0.05 g/L, $C_{TC/SMZ}$ = 8.0 mg/L). The pH values of the solution were adjusted 6.0 by using negligible volumes of 0.1-1.0 mol/L HCl or NaOH solution. The aforementioned suspensions were agitated on a shaker at each predetermined contact time point at room temperature (T= 298 K). The effect of pH on the adsorption of TC and SMZ on rGOs was conducted under the same conditions as the above adsorption kinetics except that the pH values were set over wide range from 2.0 to 11.0.

The adsorption isotherms of TC and SMZ on rGOs were carried out at pH 6.0 and 298 K using batch techniques. Briefly, the aliquot of TC and SMZ (0.5-50 mg/L) were added into rGOs, respectively. The pH of suspension was adjusted by adding negligible volumes of 0.1-1.0 mol/L HCl or NaOH solution. Then the suspensions were vigorously stirred at 298 K for 24 h. The supernatants of rGOs system were centrifuged at 12000 rpm for 20 min. The concentrations of TC and SMZ were analyzed using high-performance liquid chromatograph (Agilent 1260 Infinity; Santa Clara, CA, USA) consisting of Chemstation software, a G1311C 1260 Quat Pump and a G1314B 1260 VWD VL detector. Isocratic elution was performed under the following conditions: 0.01 mol/L oxalic acid-acetonitrile-methanol (80:16:4, V:V:V) with a wavelength of 360 nm for tetracycline;[S3] 0.05 mol/L Formic acid - acetonitrile (85:15, V:V) with a wavelength of 265 nm for sulfamethazine.[S4] The injection volume and flow rate were 20 μL and 0.7 mL/min, respectively. To take account for the effect of septum and glass wall, blank experiments were carried out separately from controls receiving the same treatment and conditions without adsorbent. Calibration curves included at least seven concentration levels over the test concentration range. Based on the obtained calibration curves, the adsorbed mass of solute was calculated by subtracting mass in aqueous solution from mass added. The each experimental data was obtained by the average values of triple parallel samples. It should be pointed out that no peaks were detected in the HPLC spectra for potential degraded/transformed products of TC and SMZ.

Charaterization. The morphologies of magnetic rGOs were characterized by SEM (JEOL JSM-6700, Tokyo, Japan) and TEM (JEOL 2010 FEG microscope). The chemical surface groups of rGOs were determined by FTIR (Nicolet 8700 FTIR spectrometer, Thermo Scientific Instrument Co. USA) equipped with a KBr beam splitter at room temperature. The mineralogy of rGOs was identified by XRD (X'Pert PRO diffractometer) with Cu Kα radiation ($\lambda = 0.154$ nm). The X-ray photoelectron spectra (XPS) were characterized by the thermo ESCALAB 250 electron spectrometer with multidetection analyzer using Al Kα X-ray source (1486.6 eV) at 10 kV and 5 mA under 10^{-8} Pa residual pressure. Surface charging effects were corrected with C 1s peak at 284.4 eV as a reference. The recorded lines were fitted by using XPSPEAK41 program after subtraction of the background (Shirley baseline correction). UV-VIS spectra were obtained by an ultraviolet–visible spectrophotometer (UV-2550, Shimadzu, Kyoto, Japan). Raman spectroscopy was carried out on an NR-1800 laser Raman spectrometer. Zeta potentials were measured using 90 Plus particle size analyzer with BI-Zeta option (Brookhaven Instruments Corporation, TX, USA). The thermal gravity analysis (TGA) of rGOs was conducted by using a Shimadzu TGA-50 thermogravimetric analyzer with an air rate of 50 ml/min. The rGOs containing TC/SMZ were collected and freeze-dried for the FTIR, UV-VIS, SEM and XPS analysis. The surface areas of rGOs were determined at -195.8 °C by nitrogen adsorption-desorption isotherms using Tristar II 3020 M (Micromeritics Co., USA).

According to Raman spectroscopy, the G band and D band of GOs and rGOs are observed (Figure S1A). Compared to GOs, the D band of rGOs is shifted from 1363 cm^{-1} to 1352 cm^{-1}, indicating the rGOs is deeper reduced (Figure S1A).[S2] The intensity ratio of the D band to the G band (I_D/I_G) ratio is used to estimate the relative extent of structural defects.[S5] The values of I_D/I_G increase from 0.92 (for GO) to 1.1 (for rGOs) after reduction, suggesting a decrease in the sp^2 carbon domains and an increase in the sp^3 carbon domains after reduction of GOs.[S2] The 2D peak position at 2650~2700 cm^{-1} indicates that the graphene layer is monolayer and bi-layer flakes.[S6] Figure S1B shows the XRD patterns of samples before and after the $H_2N\text{-}NH_2$ reduction. GOs has a sharp peak at 10.22°, and the peak completely disappears in rGOs.[S7] In XRD pattern of rGOs, the reappearance of diffraction peak at $2\theta = 25.41°$ is attributed to the rather limited ordering in each rGO nanosheet and the uneven interlayer spacing over the whole rGO sample.[S8] The rGOs were present as single layer or fewer layers from TEM (Figure S1C). As shown in Figure S1D, the specific surface area of GOs and rGOs via N_2 adsorption-desorption yielded a BET values of 81.2 and 384.5 m^2/g, respectively, which is siginfinifantly lower than the theoretical surface area for isolated graphene sheets (2620 m^2/g) due to the agglomeration of the

GOs upon reduction.[S9]

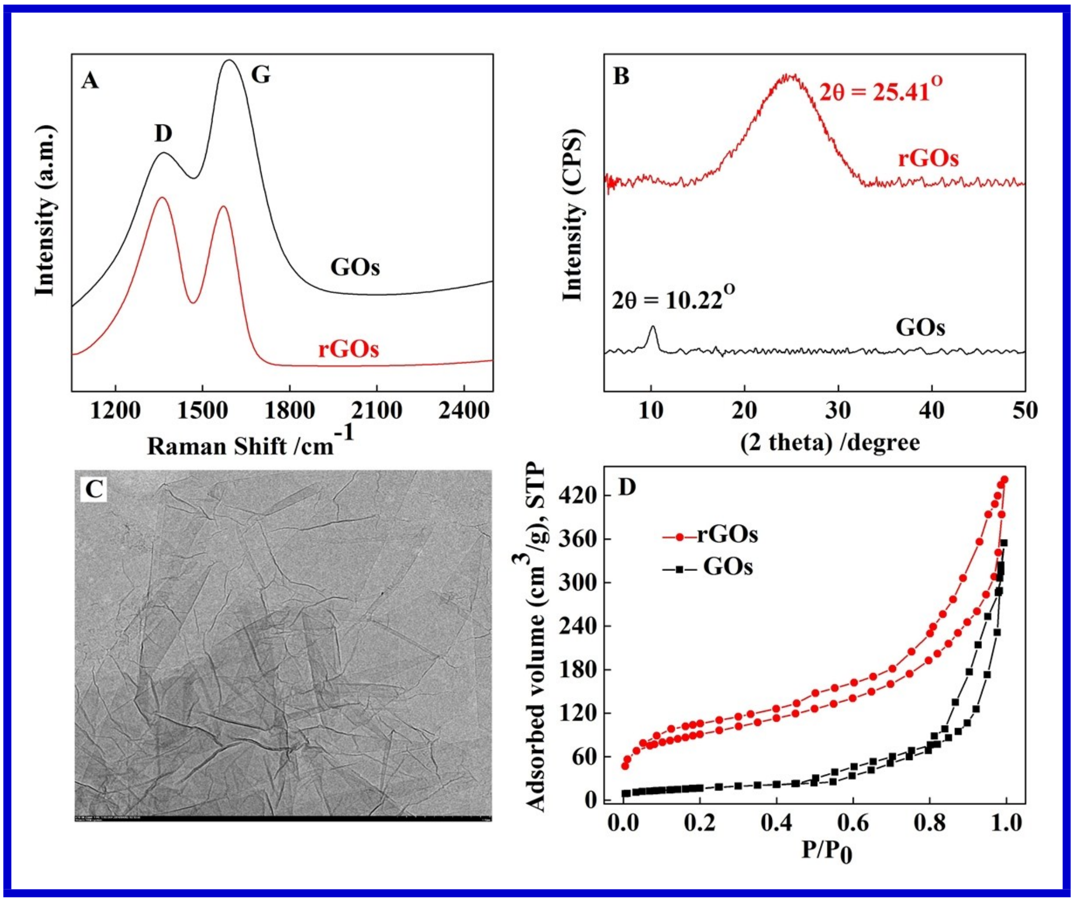

Figure S1. The characterization of rGOs, A: Raman; B: XRD; C: TEM; D: N_2-sorption and desorption curves

Distribution of TC and SMZ Species in Aqueous Solutions. The distribution of different TC and SMZ species in aqueous solutions as a function of solution pH is given in Figure S2, and selective properties of TC and SMZ used in this study is shown in Table S1**.**

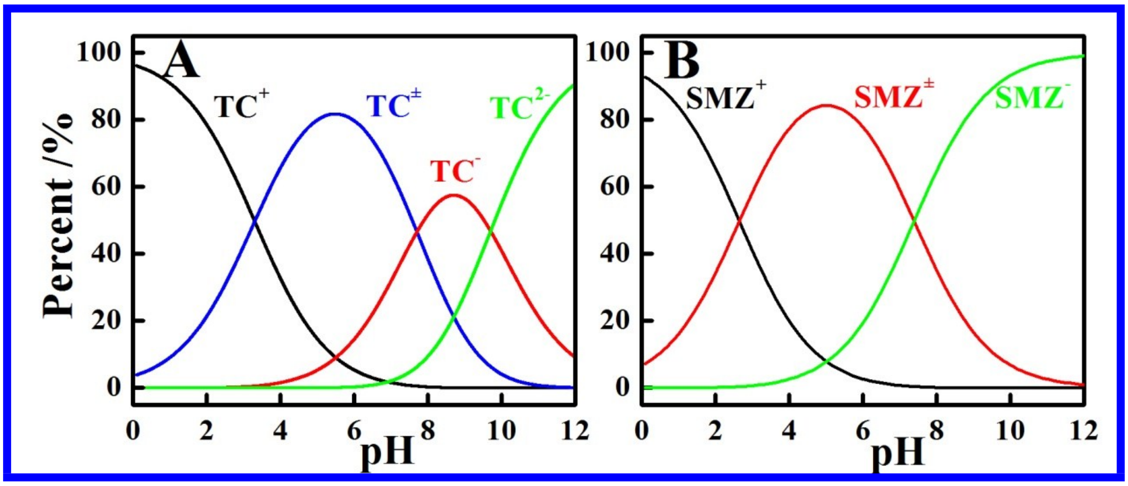

Figure S2 Species distribution as a function of pH based on the equilibrium constants.

$C_0 = 8.0$ mg/L.

Table S1. Selective properties of TC and SMZ used this study

Properties	TC[S10]	SMZ[S11]
Formula	$C_{22}H_{24}N_2O_8$	$C_{12}H_{14}N_4O_2S$
Density (g/cm^3)	1.644	1.588
Solubility in water (mg/L)	1.7	1.5
log *Kow*[a]	-1.3	1.4
pKa_1[b]	3.30	2.65
pKa_2	7.68	7.65
pKa_3	9.68	
Molecular structure	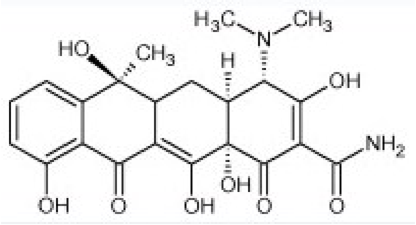	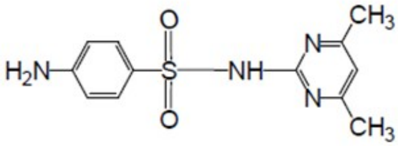

[a] Octanol-water partition coefficient, [b] Acid dissociation constants

Sorption Kinetics. The linear forms of pseudo-first-order[S12] and pseudo-second-order[S13] are given as Eqns. (S1) and (S2), respectively:

$\lg (Q_e-Q_t) = \log Q_e - k_f t/2.303$ (S1)

$t/Q_t = 1/(k_s Q_e^2) + t/Q_e$ (S2)

where Q_e and Q_t (mg/g) are the amounts of TC and SMZ adsorbed on solid phase at equilibrium and at time t, respectively, and k_f and k_s (g/(mg·h)) are the rate constants of pseudo-first-order and pseudo-second-order model, respectively.

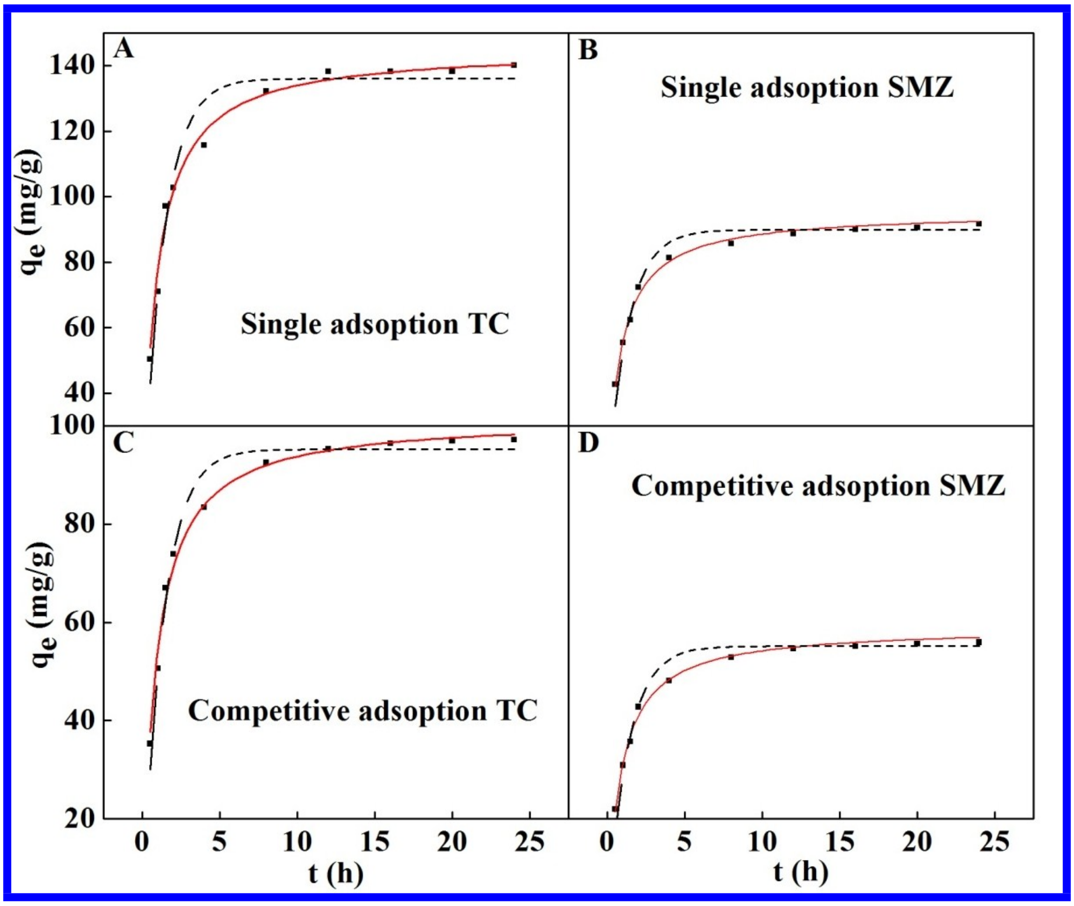

Figure S3 The fitted sorption kinetics by two models. $C_0 = 8.0$ mg/L, pH = 6.0, m/v = 0.05 g/L, T= 298 K. Black line: pseudo-first order model; Red line: pseudo-second order model.

Table S2. Parameters obtained from different kinetic models

Model		Single sorption		Competitive sorption	
		TC	SMZ	TC	SMZ
Pseudo first order	k_f (1/h)	0.204	0.177	0.196	0.164
	Q_e (mg/g)	135.49	84.80	94.84	55.126
	R^2	0.842	0.863	0.851	0.872
Pseudo second order	k_s (g/(mg·h))	3.443	0.848	3.183	0.802
	Q_e (mg/g)	144.93	89.29	101.45	50.04
	R^2	0.998	0.999	0.999	0.998

Table S3. Parameters of the Langmuir and Freundlich models of TC/SMZ on rGOs

Adsorbate		T	Langmuir model			Freundlich model		
		(K)	Q_{max} (mg/g)	b (L/mg)	R^2	K_F ($mg^{1-n}L^n/g$)	n	R^2
TC	Single sorption	298	219.10	0.0324	0.997	30.001	0.436	0.971
		318	263.82	0.0276	0.998	28.373	0.483	0.975
		338	335.73	0.0234	0.998	26.943	0.541	0.982
	Competitive sorption	298	154.58	0.0189	0.980	13.892	0.475	0.999
SMZ	Single sorption	298	174.42	0.0510	0.993	18.254	0.467	0.959
		318	202.55	0.0626	0.993	14.159	0.441	0.960
		338	229.57	0.0767	0.993	10.690	0.418	0.961
	Competitive sorption	298	123.18	0.0117	0.979	7.519	0.52413	0.999

Adsorption Isotherms. The experimental data are simulated by the Langmuir[S14] and Freundlich[S15] models:

$$C_s = b \times Q_{\max} \times C_e / (1 + b \times C_e) \qquad \text{(S3)}$$

$$C_s = K_F C_e^n \qquad \text{(S4)}$$

where C_s is the amount of antibiotics adsorbed on rGOs (mg/g), Q_{max} is the maximum amount of antibiotics adsorbed on rGOs (mg/g) at complete monolayer coverage, b (L/mg) is the Langmuir constant that relates to the sorption heat, K_F (mg^{1-n} L^n/g) represents the sorption capacity when the equilibrium concentration of antibiotics equals to 1, and *n* represents the degree of dependence of sorption with equilibrium concentration.

Table S4. Comparison of maximum adsorption capacities of TC/SMZ on various adsorbents

Sorbents	Exp. conditions	Q_{max} (mg/g)	Ref.
		TC	
Acid soils 1	pH =4.5	13.155	S16
electrocoagulation with aluminum electrodes	T = 293 K	5000	S17
Rosa canina gall extract modified polyacrylamide based cryogels	pH = 9.0, T = 293 K	53.47	S18
Graphene oxides	pH =3.6, T = 298K	313.48	S19
Carbon nanotube -3.2%O	pH =6.0, T = 298K	269.25	S20
Rectorite	pH =4.0-5.0	140	S21
rGOs	pH =6.0, T = 298 K	219.10	This study
		SMZ	
Thermal-responsive magnetic molecularly imprinted polymers	pH =7.0 , T = 298 K	3.09	S22
Thermal-responsive magnetic molecularly non-imprinted polymers	pH = 7.0, T = 298 K	1.53	S22
Molecularly imprinted polymers	pH = 4.5, T = 298 K	0.13	S23
Kaolinite	T = 298 K	79.59	S24
Soil S1 + 2% biochar-700	pH = 5.0, T = 298 K	0.315	S25
Purolite hypercrosslinked adsorbent MN250		111	S26
Molecularly imprinted microspheres	T = 298 K	13.22	S27
rGOs	pH =6.0, T = 298 K	174.42	This study

Theoretical Calculations. The optimized geometric parameters of TC and SMZ were shown in Figure S4. TC displays "L"-type structures, whereas the molecular structure of SMZ displays an arched "V" shape.

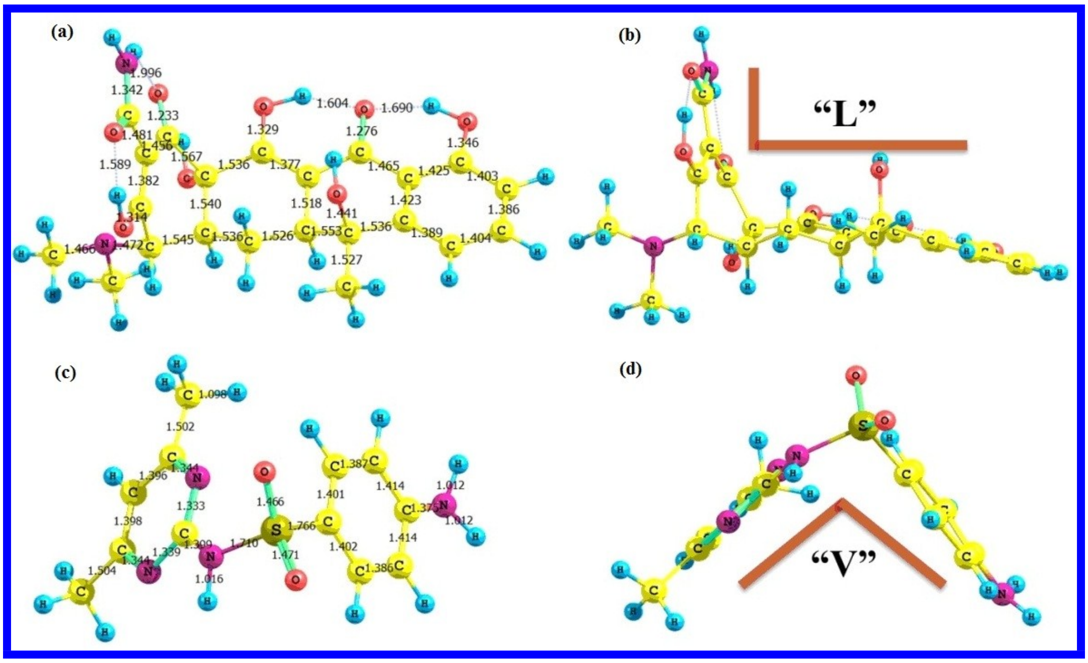

Figure S4. Optimized geometrical parameters for TC (a. top view, b. side view) and SMZ (c. top view, d. side view).

Regeneration Studies. To begin with, certain amounts of rGOs, TC and SMZ were mixed in glass vials (total 10 mL, m/v = 0.05 g/L, $C_{TC/SMZ}$ = 8.0 mg/L). The pH values of the solution were adjusted 6.0 by using negligible volumes of 0.1-1.0 mol/L HCl or NaOH solution. After achieving equilibrium, n-hexane (10 mL) was added to the reactor and stirred for 2 h. Then, n-hexane was separated from the reactor carefully and TC/SMZ in solvent was analyzed using HPLC. After the first cycle, the rGOs was separated from the solvent and reused for the subsequent adsorption and desorption cycles.

XPS Analysis. XPS C 1s spectra of rGOs, rGOs-TC and rGOs-SMZ were fitted by

XPSPEAK41 mode.

Table S5. Curve fitting results of XPS C 1s spectra of rGOs, rGOs-TC and rGOs-SMZ

Peak		BE (eV)	FWHM (eV)	%
rGOs	C=O	287.80	2.0	7.68
	C-O	286.10	1.48	13.97
	C-C	284.51	1.24	78.35
rGOs-TC	O-C=O	289.10	1.98	4.88
	C=O	287.73	1.42	3.76
	C-O	286.10	1.79	19.65
	C-C	284.74	1.13	71.71
rGOs -SMZ	O-C=O	289.1	1.094	1.08
	C=O	287.9	2.469	7.08
	C-O	286.1	1.884	19.03
	C-C	284.771	1.135	72.81

References

(S1) W. S. Hummers and R. E. Offeman, *J. Am. Chem. Soc.* 1958, 80, 1339–1339.

(S2) S. Stankovich, D. A. Dikin, R. D. Piner, K. A. Kohlhaas, A. Kleinhammes, Y. Y. Jia, Y. Wu, S. T. Nguyen and R. S. Ruoff, *Carbon*, 2007, 45, 1558–1565.

(S3) X. D. Zhu, Y. J. Wang, R. J. Sun and D. M. Zhou, *Chemosphere*, 2013, 92, 925–932.

(S4) Z. Qiang, X. Bao and W. Ben, *Water Res*., 2013, 47, 4107–4114.

(S5) H. C. Gao, F. Xiao, C. B. Ching and H. W. Duan, *ACS Appl. Mater. Inter.*, 2011, 3, 3049–3057.

(S6) Q. Wang, J. X. Li, Y. Song and X. K. Wang, *Chem. Asian J.*, 2013, 8, 225–231.

(S7) D. Long, W. Li, L. Ling, J. Miyawaki, I. Mochida and S. H. Yoon, *Langmuir*, 2010, 26, 16096–16102.

(S8) Y. B. Sun, S. B. Yang, G. X. Zhao, Q. Wang and X. K. Wang, *Chem. Asian J.* 2013, 8, 2755–2761.

(S9) S. Stankovich, D. A. Dikin, G. H. B. Dommett, K. M. Kohlhaas, E. J. Zimney, E. A. Stach, R. D. Piner, S. T. Nguyen and R. S. Ruoff, *Nature*, 2006, 442, 282–286.

(S10) Q. Zhou, Z. Li, C. Shuang, A. Li, M. Zhang and M. Wang, *Chem. Eng. J.*, 2012, 210, 350–356.

(S11) W. Gong, X. Liu, H. He, L. Wang, and G. Dai, *Chemosphere*, 2012, 89, 825–831.

(S12) S. Lagergren, *Kungl. Svenska Vetenskapsakad. Handl.*, 1898, 24, 1–39.

(S13) Y.S. Ho and G. McKay, *Proc. Saf. Environ. Prot.*, 1998, 76, 183–191.

(S14) I. Langmuir, *J. Am. Chem. Soc.* 1918, 40, 1361–1403.

(S15) H. M. F. Freundlich, *J. Phys. Chem.*, 1906, 57, 385–470.

(S16) D. Fernández-Calviño, A. Bermúdez-Couso, M. Arias-Estévez, J. C. Nóvoa-Muñoz, M. J. Fernández-Sanjurjo, E. Álvarez-Rodríguez and A. Núñez-Delgado, *Environ. Sci. Pollut. Res.*, 2015, 22, 425–433.

(S17) Y. A. Ouaissa, M. Chabani, A. Amrane, and A. Bensmaili, *J. Environ. Chem. Eng.*, 2014, 2, 177–184.

(S18) E. Bağda, M. Erşan and E. Bağda, *J. Environ. Chem. Eng.*, 2013, 1, 1079–1084.

(S19) Y. Gao, Y. Li, L. Zhang, H. Huang, J. Hu, S. M. Shah and X. Su, *J. Colloid Interf. Sci.*, 2012, 368, 540–546.

(S20) F. Yu, J. Ma and S. Han, *SCI. REP-UK.*, 2014, 4, 1 – 8.

(S21) P. H. Chang, J. S. Jean, W. T. Jiang and Z. Li, *Colloid Surface A,* 2009, 339, 94–99.

(S22) L. Xu, J. Pan, J. Dai, X. Li, H. Hang, Z. Cao and Y. Yan, *J. Hazard. Mater.*, 2012, 233, 48–56.

(S23) L. Chen, X. Zhang, L. Sun, Y. Xu, Q. Zeng, H. Wang, H. Xu, A. Yu, H. Zhang, and L. Ding, *J. Agric. Food Chem.*, 2009, 57, 10073–10080.

(S24) J. Xu, Y. He, Y. Zhang, C. Guo, L. Li and Y. Wang, *Front. Env. Sci. Eng.*, 2013, 7, 836–843.

(S25) M. Vithanage, A. U. Rajapaksha, X. Tang, S. Thiele-Bruhn, K. H. Kim, S. E. Lee and Y. S. Ok, *J. Environ. Manage.*, 2014, 141, 95–103.

(S26) M. E. Grimmett, *J. Environ. Qual.*, 2013, 42, 2–9.

(S27) J. Dai, Y. Zou, Z. Zhou, X. Dai, J. Pan, P. Yu and C. Li, *RSC Adv.*, 2014, 4, 1965–1973.